<u>**Supplemental Figure Legends**</u>

Figure S1. CoQ-deficient mice show histologic evidence of kidney injury at five months.

A. Electron micrographs of kidneys of CTRL and KDKD mice show diffuse podocyte foot process effacement (arrowheads) in glomeruli of KDKD mice; Pod, podocyte; PEC, parietal epithelial cell; Mes, mesangial cell; EC, endothelial cell; RBC, red blood cell; CL, capillary lumen; BS, Bowman's space; FP, podocyte foot processes. **B, C.** Quality control measures of sNuc-Seq by sample. **D.** UMAP visualization of single nucleus transcriptomic profiles from three five-month-old *Pdss2*$^{kd/kd}$ mice (KDKD) and three age-matched control mice (CTRL) color-coded by sample.

Figure S2. sNuc-Seq of CoQ-deficient and age-control mice retrieve all expected major kidney cell types.

Violin plot representation of gene expression of canonical marker genes for different kidney cell types across all clusters.

Figure S3. sNuc-Seq of CoQ-deficient and age-control mice reveal disease-specific populations.

A. Proportions of clusters by sample (left) with corresponding cell numbers (right). **B.** Violin plot expression of TAL (*Slc12a1*), DCT (*Slc12a3*) canonical markers with *Dcdc2a* (top), and expression of three genes by UMAP representation only in Mixed–TAL/DCT cluster (bottom).

Figure S4. *Dock10/Vcam1*+ PEC population identified in CoQ-deficient mice.

A. Volcano plot of genes based on enrichment in *Dock10/Vcam1*+ cluster colored by significance (black, p-adj. < 0.05, Wilcox rank sum test) and selected genes (red). **B.** Dot plot representation of gene expression of canonical marker genes for parietal epithelial cells (PECs). Note *Dock10/Vcam1*+ cells uniquely co-express the PEC markers *CD44*, *Pax8* and *Cldn1*. **C.** Correlation plot of average gene expression across clusters show *Dock10/Vcam1*+ cells most similar to proximal tubule (PT) cells. **D.** Immunofluorescence staining for PT (Lrp2) and Vcam1 in CTRL versus KDKD mice shows increased Vcam1 expression in KDKD (left; scale bars, 500 m). Higher magnification shows Vcam1 co-localization with Lrp2+ PT cells (right; scale bars, 50 m). **E.** Immunofluorescence staining for podocytes (Synpo) and Vcam1 in CTRL versus KDKD mice shows BC localization surrounding Synpo+ glomeruli; scale bars, 50 m. **F.** *In situ* hybridization chain reaction shows co-localization of Dock10 and Vcam1 mRNA in cells surrounding podocytes (Nphs2), scale bars, 20 m. **G.** Immunofluorescence staining for podocytes (Synpo), PEC activation (Cd44) and Vcam1 in KDKD mice shows BC and PEC localization surrounding Synpo+ glomeruli; scale bars, 50 m. **H.** Immunofluorescence staining for podocytes (Synpo), PEC activation (Cd44) and PECs (Cldn1) in CTRL versus KDKD mice shows BC localization of Cldn1+ PECs surrounding Synpo+ glomeruli with Cd44 PEC-activation only in KDKD mice; scale bars, 50 m.

Figure S5. Podocytes in Pdss2$^{kd/kd}$ mice have podocyte injury, increased ETC expression and proteinuria by four months of age.

A. Periodic acid–Schiff (PAS) staining of kidneys from CTRL and KDKD mice showing proteinuric casts in tubules of KDKD mice (*) and activation of PECs (arrowheads) at higher magnification, as seen by increased numbers and more prominent nucleoli. **B.** Gene expression of canonical podocyte marker genes (Synaptopodin (Synpo), Wt1, Plce1) in podocytes from control and *Pdss2$^{kd/kd}$* mice. **C.** Heatmap of average gene expression of electron transport genes (Complex I-IV) across podocyte and combined proximal tubules cells in CTRL versus KDKD mice. **D.** Average age of animals used for GDC-0879 treatment (top) and day 1 proteinuria levels (bottom).

Figure S6. Pdss2 knockdown in podocytes leads to CoQ deficiency but no alteration in known CoQ functions.

A. Western blot from Pdss2 shRNA infected podocytes or scrambled controls five days post-lentivirus infection. **B.** Log2 fold change of CoQ levels (CoQ9 and CoQ10) in Pdss2 shRNA infected podocytes compared to scrambled controls, n=4. **C,D.** Mito-stress test to assess electron transport chain (ETC) function by oxygen consumption rate (OCR, top) and glycolysis by extracellular acidification rate (ECAR, bottom) with the Seahorse Flux Analyzer in Pdss2 shRNA infected podocytes and scrambled controls in **C.** full RPMI media (11.1 mM glucose) or **D.** glucose-free RPMI. **E.** Log2 fold change of uridine levels in Pdss2 shRNA infected podocytes compared to scrambled controls, n=4. **F.** Transition pore opening as measured by Calcein-AM in the presence of $CoCl_2$, normalized to total mitochondrial abundance, measured by MitoTracker Deep Red in Pdss2 shRNA infected podocytes and scrambled controls, n=4, one-way ANOVA, Tukey multiple comparison test. **G.** Cellular ROS as measured by the sum fluorescence

of CellROX Orange dye in Pdss2-depleted podocytes and scrambled controls, n=4, one-way ANOVA, Tukey multiple comparison test.

Figure S7. Metabolomics of Pdss2-depleted podocytes show increased abundance of polyunsaturated triglycerides and decreased abundance of polyunsaturated phospholipids.

A. Heatmap of statistically significant metabolites (FDR <10%, Benjamini-Hochberg correction on a student's t-test) from cell extracts of Pdss2 shRNA infected podocytes compared to scrambled controls, n=4. **B.** Lipidomic analysis across 14 lipid classes demonstrate significant changes in plasmalogens, sphingomyelin, and triglycerides between Pdss2 shRNA infected podocytes compared to scrambled controls. CE, cholesterol ester; DAG, diacylglyceride; LPC, lyso-phosphocholine; LPE, lyso-phosphoethanolamine; MAG, monoacylglyceride; PC, phosphocholine; PE, phosphoethanolamine; PI, phosphoinositol; PL, phospholipid; PS, phosphoserine; SM, sphingomyelin; TAG, triacylglyceride. **C.** Log2 fold changes of sum of abundances of triglycerides sub-divided based on degree of saturation in Pdss2-depleted podocytes compared to scrambled controls.

Figure S8. GGdP increases Rar-mediated transcription in a dose-responsive manner, CoQ-deficient mice reveal podocyte-specific changes in PUFA-related genes, and Gpx4 immunofluorescence quantification.

Luminescence readout from a Retinoic Acid Receptor Element (RARE)-luciferase reporter assay following 24 hours treatment with **A.** atRA, n=3 or **B.** GGdP, n=6,

showing that both increase Rar-mediated transcription in a dose-responsive manner. **C.** Western blot of phospho-ERK1/2 (P-ERK1/2) and total ERK1/2 which shows decreased ERK1/2 phosphorylation following treatment with thapsigargin (2.5 M) and reversed with GDC-0879 (10 M). **D.** Heatmap of average gene expression of genes used to create PUFA transcriptomic signatures in original dataset of 61 free fatty acids in MIN6 cells, demonstrating selected genes are either up- or down-regulated specifically among PUFAs. **E.** Heatmap of average gene expression of genes used to create the PUFA upregulated gene signature (PUFA up) and PUFA downregulated gene signature (PUFA down) across podocyte and combined proximal tubule cells in control versus *Pdss2^{kd/kd}* mice.

Figure S9. Image analysis using Opera Phenix High-Content Screening System and Harmony software.

A. Analysis of immunofluorescence by Harmony software demonstrating identification of glomeruli, based on Synpo expression, and surrounding regions for Gpx4 quantification. **B.** Immunofluorescence of synaptopodin (Synpo, red) with nuclei staining (DAPI, blue) and quantification by cell size showing larger cells have increased expression of synaptopodin (SYNPO) suggesting further podocyte maturation; scale bars, 100 m. **C.** Analysis of live cell imaging by Harmony software demonstrating identification of cell bodies, selection of cells based on size, and selection of apoptotic (caspase positive) and dead cells. **D.** Dose-response curve for GDC-0879 inhibition of podocyte apoptosis in vitro, n=4, IC50 for each condition determined using a nonlinear least squares fit.

Supplementary Tables

Supplementary Table 1: Marker gene lists for all identified clusters

Supplementary Table 2: Differential expression (DE) list and gene set enrichment analysis (GSEA) on CTRL versus KDKD podocyte DE

Supplementary Table 3: Metabolomics data and differential abundance (DA) analysis for all annotated metabolites from conditioned media and cell lysates for scrambled controls and Pdss2

Supplementary Table 4: Differential expression (DE) and gene set enrichment analysis (GSEA) of bulk RNA-seq data comparing scrambled controls and Pdss2 shRNAs

Supplementary Table 5: Metabolomics data and differential abundance (DA) analysis for all detected metabolites from conditioned media with atRA treatement versus DMSO control

Supplementary Table 6: Product information for reagents, antibodies, and primer sequences
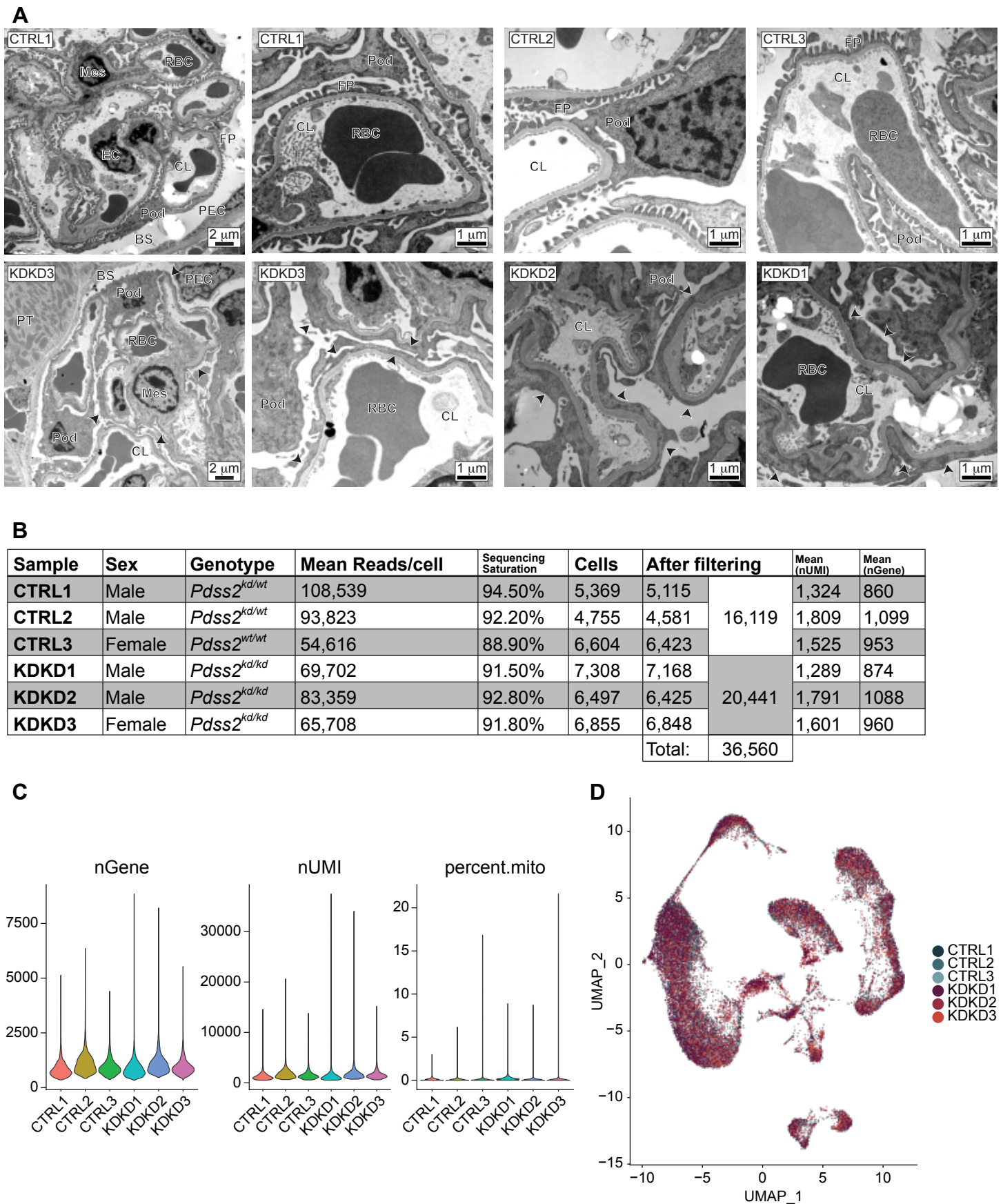
A

B

Sample	Sex	Genotype	Mean Reads/cell	Sequencing Saturation	Cells	After filtering		Mean (nUMI)	Mean (nGene)
CTRL1	Male	*Pdss2*$^{kd/wt}$	108,539	94.50%	5,369	5,115		1,324	860
CTRL2	Male	*Pdss2*$^{kd/wt}$	93,823	92.20%	4,755	4,581	16,119	1,809	1,099
CTRL3	Female	*Pdss2*$^{wt/wt}$	54,616	88.90%	6,604	6,423		1,525	953
KDKD1	Male	*Pdss2*$^{kd/kd}$	69,702	91.50%	7,308	7,168		1,289	874
KDKD2	Male	*Pdss2*$^{kd/kd}$	83,359	92.80%	6,497	6,425	20,441	1,791	1088
KDKD3	Female	*Pdss2*$^{kd/kd}$	65,708	91.80%	6,855	6,848		1,601	960
						Total:	36,560		

C

D

Figure S1. CoQ-deficient mice show histologic evidence of kidney injury at five months.
A. Electron micrographs of kidneys of CTRL and KDKD mice show diffuse podocyte foot process effacement (arrowheads) in glomeruli of KDKD mice; Pod, podocyte; PEC, parietal epithelial cell; Mes, mesangial cell; EC, endothelial cell; RBC, red blood cell; CL, capillary lumen; BS, Bowman's space; FP, podocyte foot processes. **B, C.** Quality control measures of sNuc-Seq by sample. **D.** UMAP visualization of single nucleus transcriptomic profiles from three five month old *Pdss2*$^{kd/kd}$ mice (KDKD) and three age-matched control mice (CTRL) color-coded by sample.
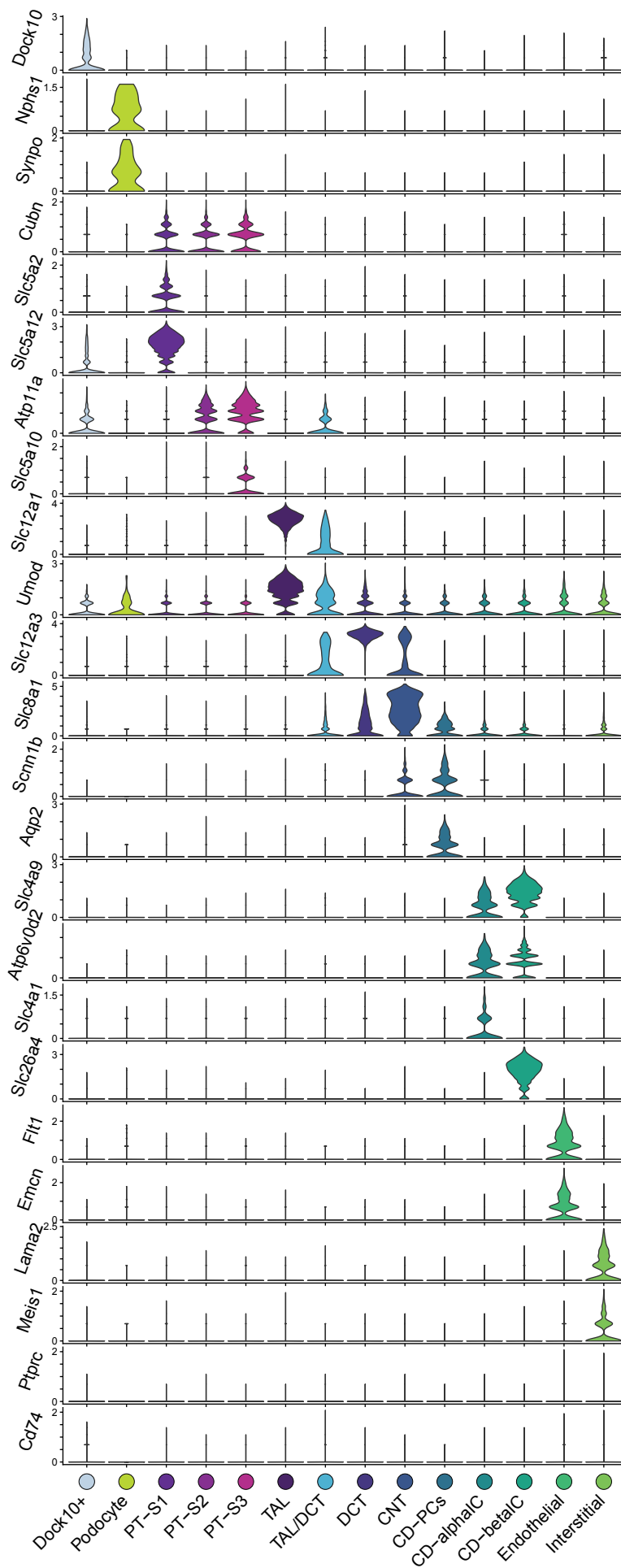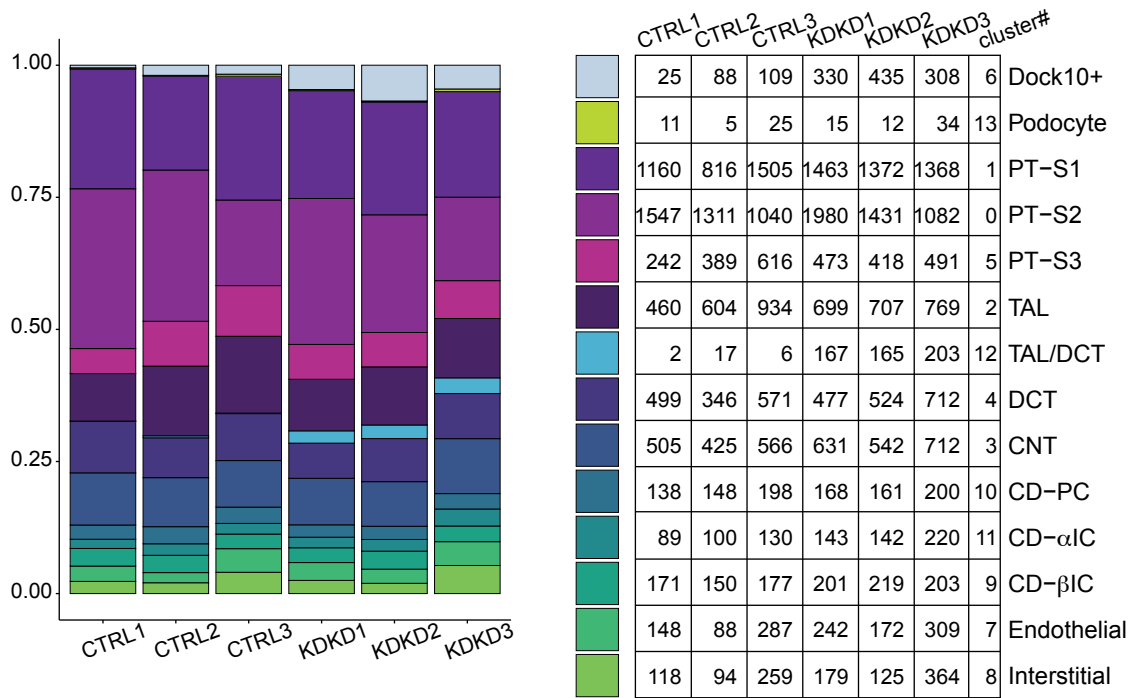
Figure S2. sNuc-Seq of CoQ-deficient and age-control mice retrieve all expected major kidney cell types.
Violin plot representation of gene expression of canonical marker genes for different kidney cell types across all clusters.
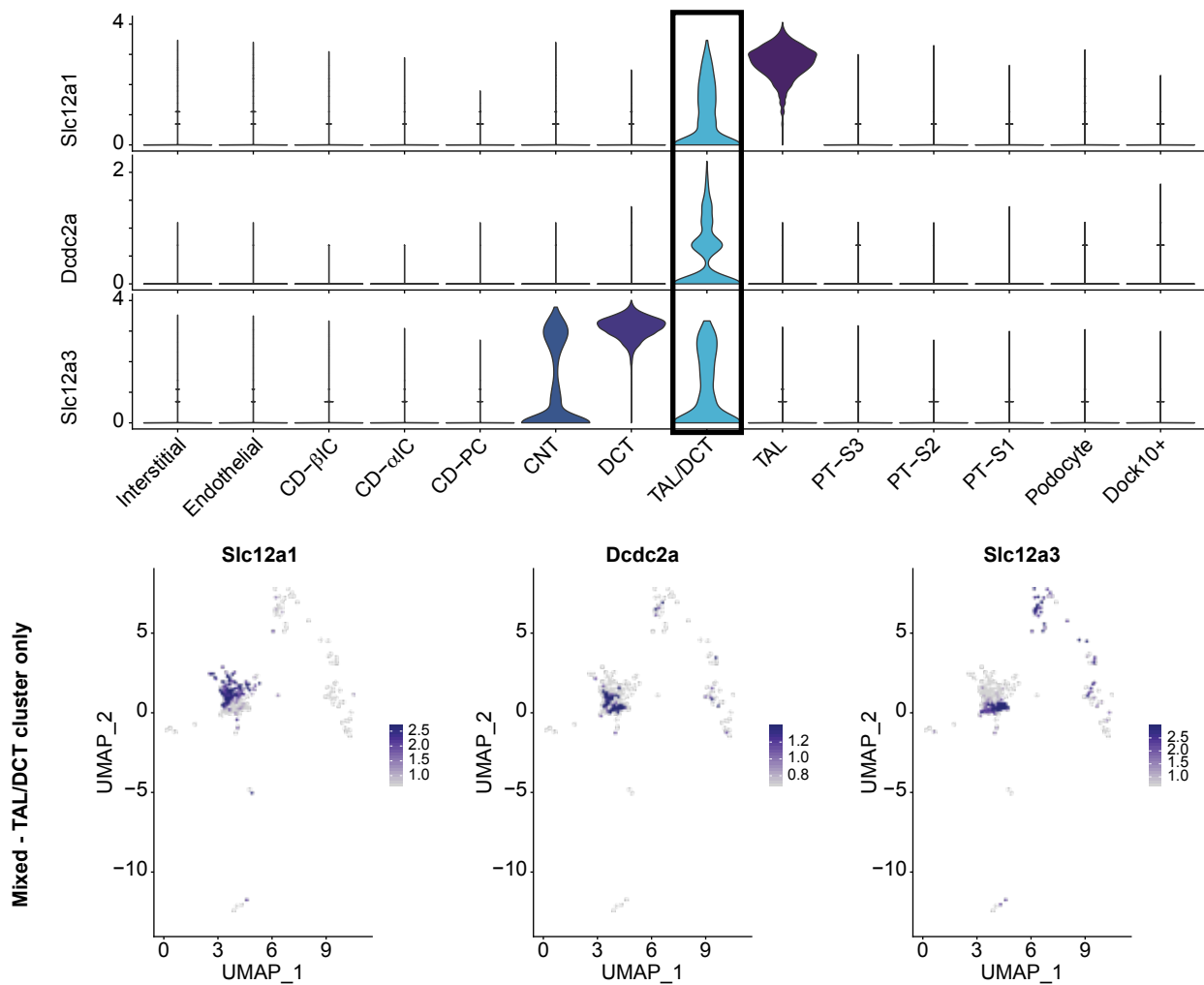
A

	CTRL1	CTRL2	CTRL3	KDKD1	KDKD2	KDKD3	cluster#	
	25	88	109	330	435	308	6	Dock10+
	11	5	25	15	12	34	13	Podocyte
	1160	816	1505	1463	1372	1368	1	PT−S1
	1547	1311	1040	1980	1431	1082	0	PT−S2
	242	389	616	473	418	491	5	PT−S3
	460	604	934	699	707	769	2	TAL
	2	17	6	167	165	203	12	TAL/DCT
	499	346	571	477	524	712	4	DCT
	505	425	566	631	542	712	3	CNT
	138	148	198	168	161	200	10	CD−PC
	89	100	130	143	142	220	11	CD−αIC
	171	150	177	201	219	203	9	CD−βIC
	148	88	287	242	172	309	7	Endothelial
	118	94	259	179	125	364	8	Interstitial

B

Figure S3. sNuc-Seq of CoQ-deficient and age-control mice reveal disease-specific populations.
A. Proportions of clusters by sample (left) with corresponding cell numbers (right). **B.** Violin plot expression of TAL (Slc12a1), DCT (Slc12a3) canonical markers with Dcdc2a (top), and expression of three genes by UMAP representation only in Mixed–TAL/DCT cluster (bottom).
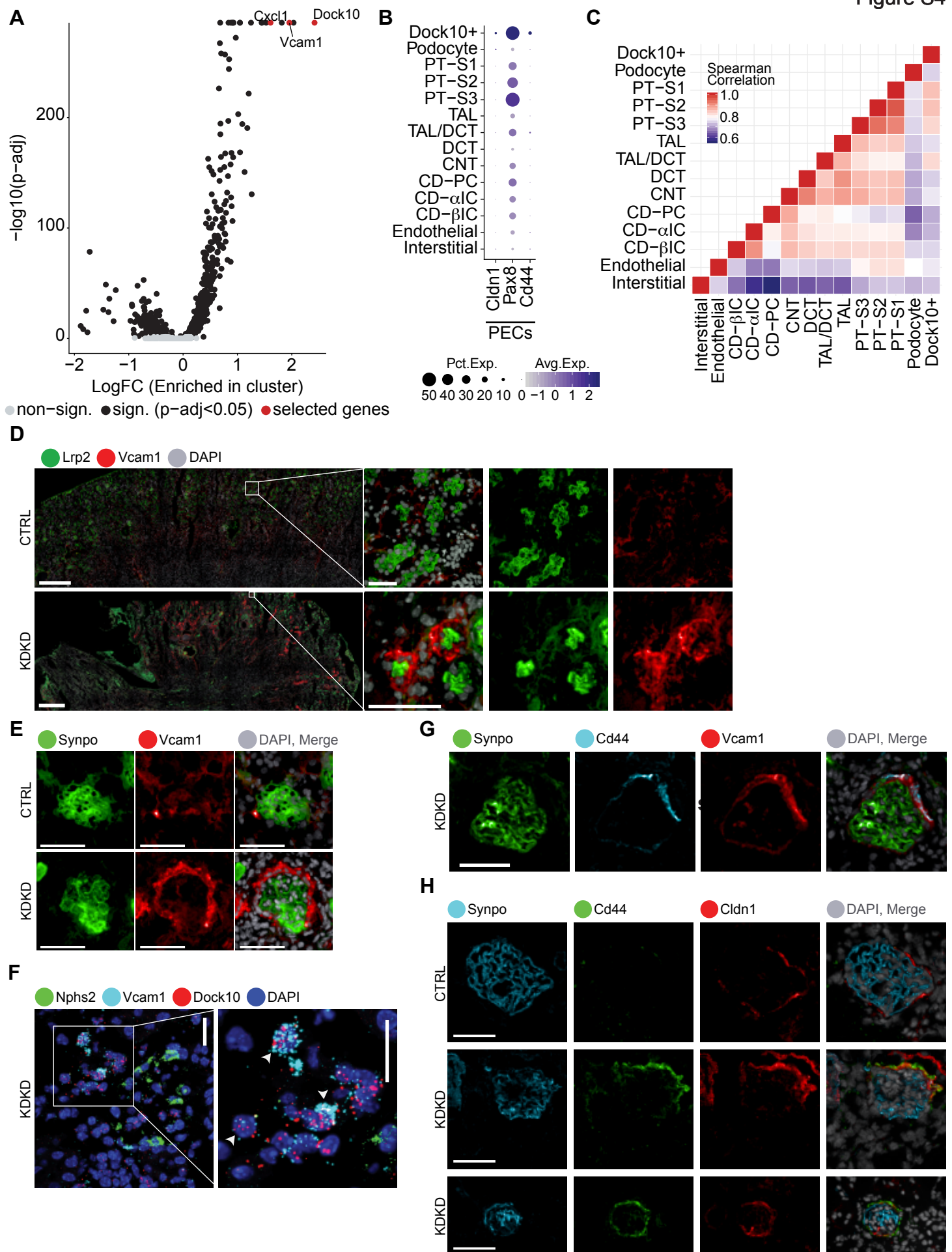
Figure S4. Dock10/Vcam1+ PEC population identified in CoQ-deficient mice.
A. Volcano plot of genes based on enrichment in Dock10/Vcam1+ cluster colored by significance (black, p-adj. < 0.05, Wilcox rank sum test) and selected genes (red). **B.** Dot plot representation of gene expression of canonical marker genes for parietal epithelial cells (PECs). Note Dock10/Vcam1+ cells uniquely co-express the PEC markers CD44, Pax8 and Cldn1. **C.** Correlation plot of average gene expression across clusters show Dock10/Vcam1+ cells most similar to proximal tubule (PT) cells. **D.** Immunofluorescence staining for PT (Lrp2) and Vcam1 in CTRL versus KDKD mice shows increased Vcam1 expression in KDKD (left; scale bars, 500 μm). Higher magnification shows Vcam1 co-localization with Lrp2+ PT cells (right; scale bars, 50 μm). **E.** Immunofluorescence staining for podocytes (Synpo) and Vcam1 in CTRL versus KDKD mice shows BC localization surrounding Synpo+ glomeruli; scale bars, 50 μm. **F.** In situ hybridization chain reaction shows co-localization of Dock10 and Vcam1 mRNA in cells surrounding podocytes (Nphs2), scale bars, 20 μm. **G.** Immunofluorescence staining for podocytes (Synpo), PEC activation (Cd44) and Vcam1 in KDKD mice shows BC and PEC localization surrounding Synpo+ glomeruli; scale bars, 50 μm. **H.** Immuno-fluorescence staining for podocytes (Synpo), PEC activation (Cd44) and PECs (Cldn1) in CTRL versus KDKD mice shows BC localization of Cldn1+ PECs surrounding Synpo+ glomeruli with Cd44 PEC-activation only in KDKD mice; scale bars, 50 μm.
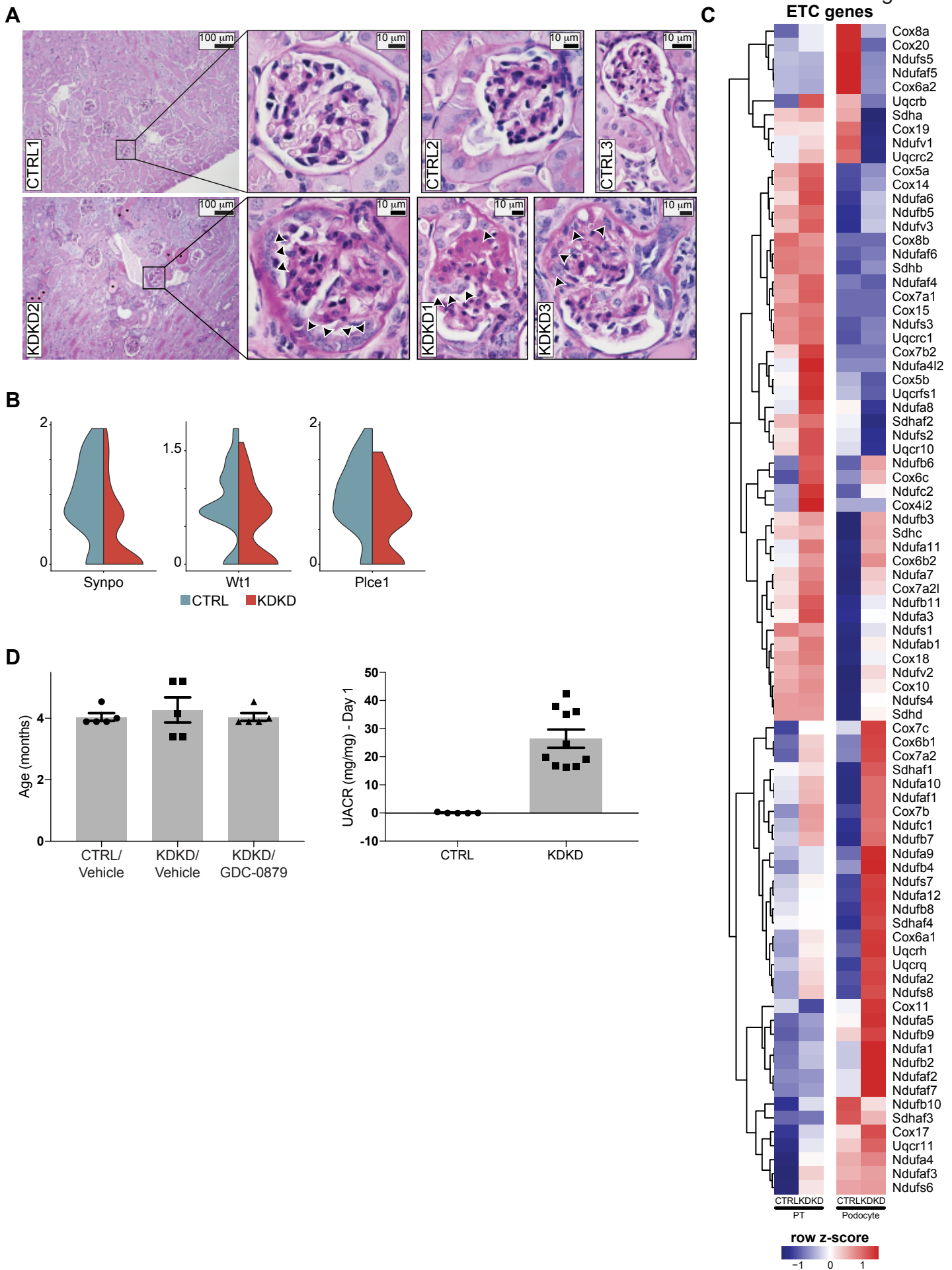
Figure S5. Podocytes in *Pdss2^kd/kd* mice have podocyte injury, increased ETC expression and proteinuria by four months of age.
A. Periodic acid–Schiff (PAS) staining of kidneys from CTRL and KDKD mice showing proteinuric casts in tubules of KDKD mice (*) and activation of PECs (arrowheads) at higher magnification, as seen by increased numbers and more prominent nucleoli. **B.** Gene expression of canonical podocyte marker genes (Synaptopodin (Synpo), Wt1, Plce1) in podocytes from control and *Pdss2^kd/kd* mice. **C.** Heatmap of average gene expression of electron transport genes (Complex I-IV) across podocyte and combined proximal tubules cells in CTRL versus KDKD mice. **D.** Average age of animals used for GDC-0879 treatment (top) and day 1 proteinuria levels (bottom).
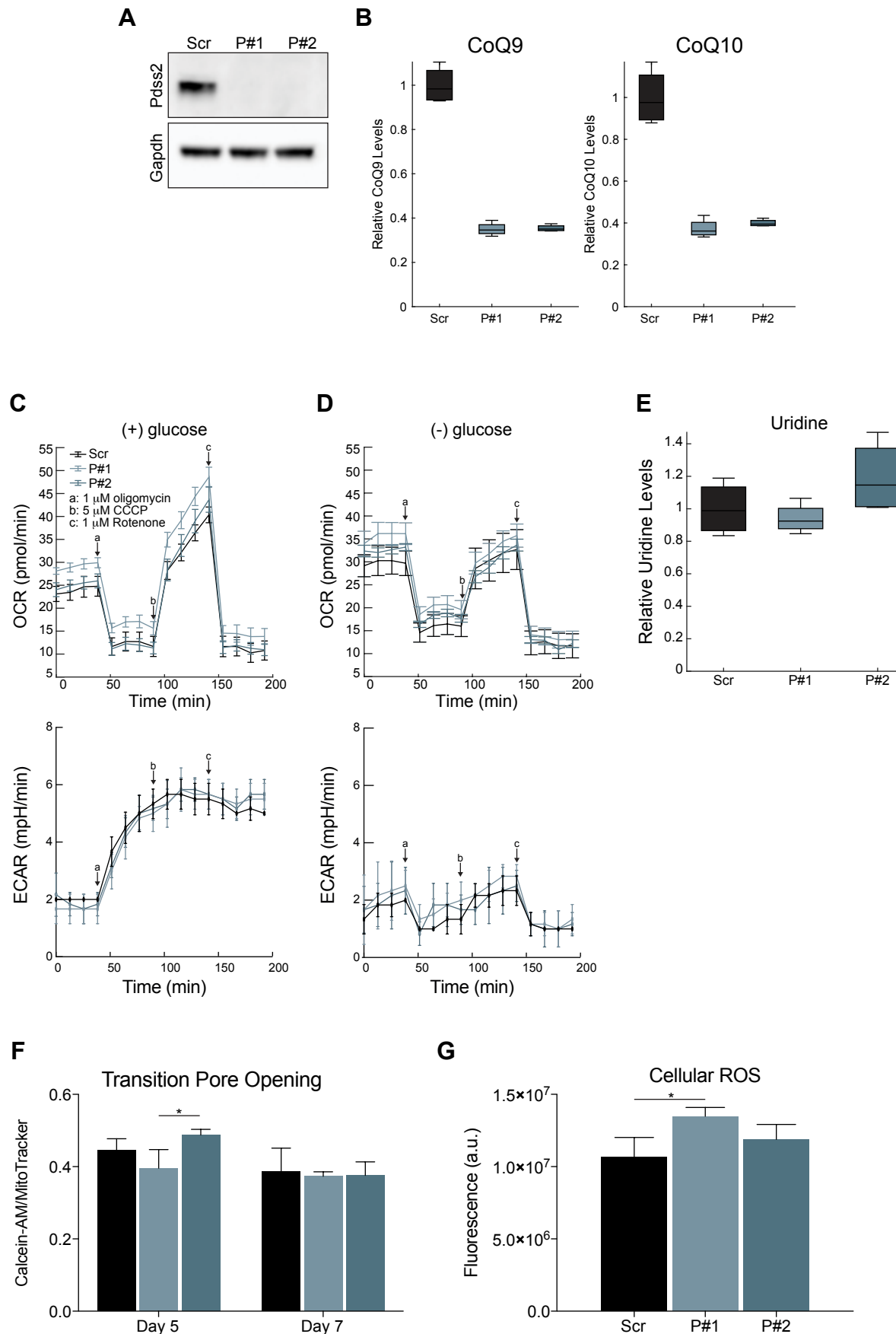
Figure S6. Pdss2 knockdown in podocytes leads to CoQ deficiency but no alteration in known CoQ functions.
A. Western blot from Pdss2 shRNA infected podocytes or scrambled controls five days post-lentivirus infection. **B.**
Log2 fold change of CoQ levels (CoQ9 and CoQ10) in Pdss2 shRNA infected podocytes compared to scrambled
controls, n=4. **C,D.** Mito-stress test to assess electron transport chain (ETC) function by oxygen consumption rate
(OCR, top) and glycolysis by extracellular acidification rate (ECAR, bottom) with the Seahorse Flux Analyzer in Pdss2
shRNA infected podocytes and scrambled controls in **C.** full RPMI media (11.1 mM glucose) or **D.** glucose-free RPMI.
E. Log2 fold change of uridine levels in Pdss2 shRNA infected podocytes compared to scrambled controls, n=4. **F.**
Transition pore opening as measured by Calcein-AM in the presence of CoCl¬2, normalized to total mitochondrial
abundance, measured by MitoTracker Deep Red in Pdss2 shRNA infected podocytes and scrambled controls, n=4,
one-way ANOVA, Tukey multiple comparison test. **G.** Cellular ROS as measured by the sum fluorescence of CellROX
Orange dye in Pdss2-depleted podocytes and scrambled controls, n=4, one-way ANOVA, Tukey multiple comparison
test.

A **Cell Metabolomics**

C58:10 TAG
NH4_C56:9 TAG
NH4_C58:8 TAG
NH4_C58:10 TAG
C58:8 TAG
C56:8 TAG
C58:9 TAG
glycolithocholate
N−Oleoylethanolamine
C5 carnitine
glycochenodeoxycholate
taurochenodeoxycholate
NH4_C58:9 TAG
beta−alanine
C58:7 TAG
NH4_C52:6 TAG
NH4_C52:5 TAG
NH4_C58:8 TAG
C54:7 TAG
NH4_C50:4 TAG
1−methylnicotinamide
C46:3 TAG
C54:5 TAG
NH4_C54:5 TAG
NH4_C56:7 TAG
N−acetylaspartic acid
C50:4 TAG
C52:5 TAG
C18:1 carnitine
C2 carnitine
C36:2 PE
C53:3 TAG
NH4_C55:2 TAG
NH4_C55:3 TAG
C54:1 TAG
NH4_C52:1 TAG
C50:1 TAG
C51:2 TAG
C54:4 TAG
NH4_C53:2 TAG
NH4_C56:4 TAG
NH4_C52:2 TAG
C56:4 TAG
NH4_C50:1 TAG
NH4_C51:1 TAG
NH4_C51:2 TAG
C50:0 TAG
NH4_C50:0 TAG
C52:1 TAG
C54:2 TAG
C55:2 TAG
C56:5 TAG
NH4_C52:4 TAG
NH4_C54:6 TAG
NH4_C58:6 TAG
C58:6 TAG
NH4_C54:4 TAG
NH4_C56:5 TAG
NH4_C56:6 TAG
C51:1 TAG
C53:2 TAG
C56:7 TAG
C54:6 TAG
C56:6 TAG
hypotaurine
taurine
C51:0 TAG
NH4_C49:0 TAG
C49:1 TAG
NH4_C49:1 TAG
C14:0 CE
C20:3 CE
alpha−glycerophosphocholine
C34:0 PE
coenzyme Q10
coenzyme Q9
C38:6 PE plasmalogen
C34:3 PC plasmalogen
C36:5 PC plasmalogen
C30:0 PC
C38:6 PC plasmalogen
C32:0 PC
C16:0 SM
C38:6 PC plasmalogen
C40:7 PE plasmalogen
C24:0 Ceramide (d18:1)
C40:7 PC plasmalogen
C30:1 PC
C34:4 PC plasmalogen
NH4_C34:2 DAG
C34:1 PC plasmalogen−A
C36:5 PC plasmalogen−B
C36:1 DAG
NH4_C36:1 DAG
alpha−ketoglutarate
oxalate
C34:4 PC
C16:0 SM
C38:7 PE plasmalogen
C18:2 SM
C22:0 SM
C24:1 SM
C46:4 TAG
C48:5 TAG
mesaconate
C38:3 PE plasmalogen
2−hydroxyglutarate
C22:5 CE
NH4_C22:4 CE
C22:4 CE
C42:11 PE plasmalogen
NH4_C22:5 CE
C24:0 SM
C38:7 PE plasmalogen

Scr   P#1   P#2

row z−score
−2   2

B

CE
Ceramide
DAG
LPC
LPE
MAG
PC
PE
PI
PL
plasmalogen
PS
SM
TAG

row z−score
2
0
−2

Scr   P#2   P#1

Statistics Summary

	Scr-P1	Scr-P2	P1-P2
CE	0.831	0.107	0.252
Ceramide	1.1E-6	0.172	3E-7
DAG	0.410	0.171	0.799
LPC	0.709	0.201	0.555
LPE	0.932	0.504	0.712
MAG	0.361	0.609	0.089
PC	1.33E-4	0.856	2.42E-4

	Scr-P1	Scr-P2	P1-P2
PE	4.17E-5	0.184	3.23E-4
PI	0.412	0.0402	0.296
PL	1.15E-3	0.814	2.25E-3
plasmalogen	2E-7	4.49E-4	1.03E-5
PS	0.0712	5.63E-4	3.56E-5
SM	2.31E-4	5.18E-5	0.372
TAG	3.09E-4	4.9E-6	4.58E-3

C   TG by sat: Log2FC

row z−score
1
0
−1

Saturated
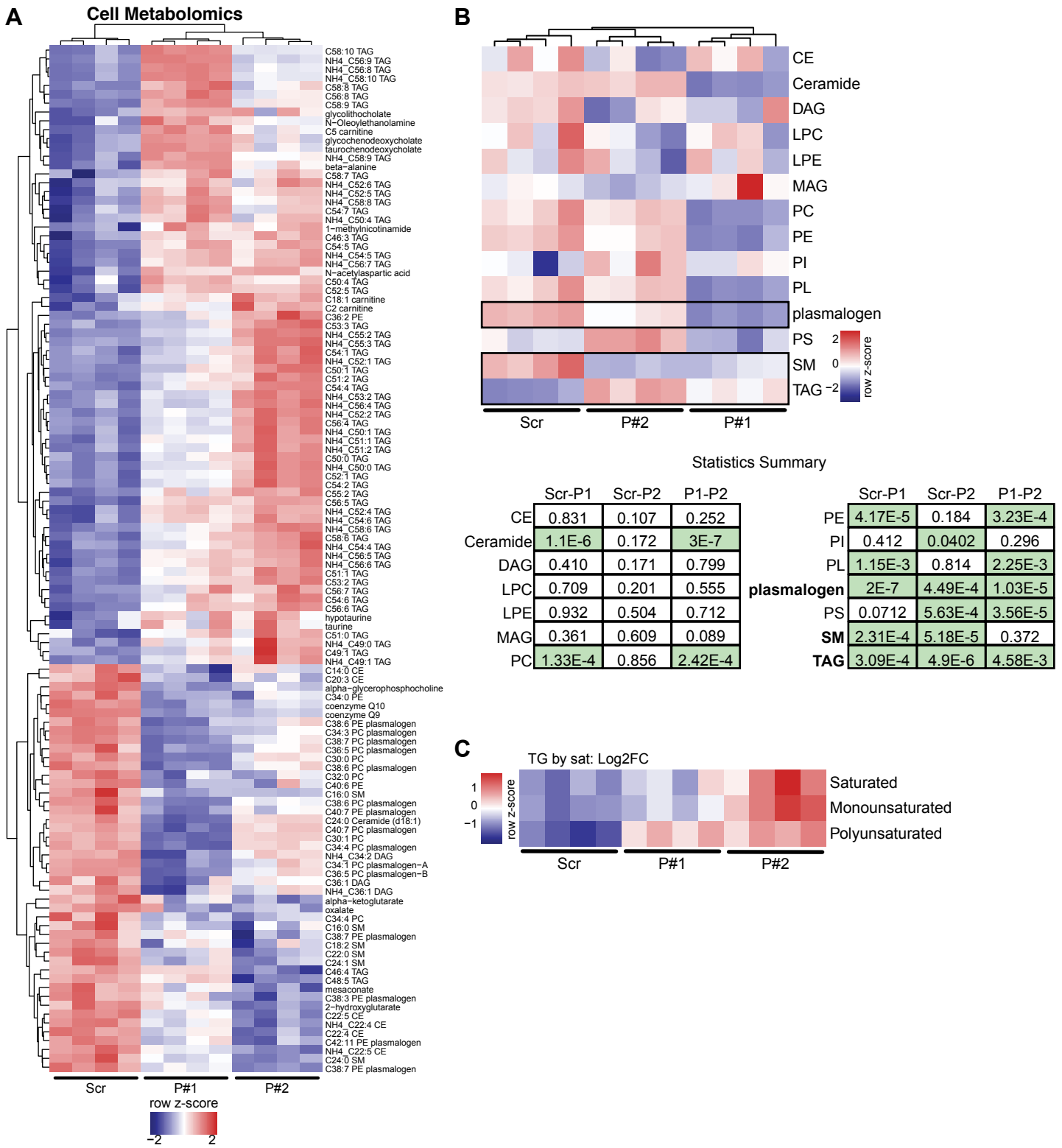Monounsaturated
Polyunsaturated

Scr   P#1   P#2

Figure S7. Metabolomics of Pdss2-depleted podocytes show increased abundance of polyunsaturated triglycerides and decreased abundance of polyunsaturated phospholipids.
A. Heatmap of statistically significant metabolites (FDR <10%, Benjamini-Hochberg correction on a student's t-test) from cell extracts of Pdss2 shRNA infected podocytes compared to scrambled controls, n=4. **B.** Lipidomic analysis across 14 lipid classes demonstrate significant changes in plasmalogens, sphingomyelin, and triglycerides between Pdss2 shRNA infected podocytes compared to scrambled controls. CE, cholesterol ester; DAG, diacylglyceride; LPC, lyso-phosphocholine; LPE, lyso-phosphoethanolamine; MAG, monoacylglyceride; PC, phosphocholine; PE, phosphoethanolamine; PI, phosphoinositol; PL, phospholipid; PS, phosphoserine; SM, sphingomyelin; TAG, triacylglyceride. **C.** Log2 fold changes of sum of abundances of triglycerides sub-divided based on degree of saturation in Pdss2-depleted podocytes compared to scrambled controls.
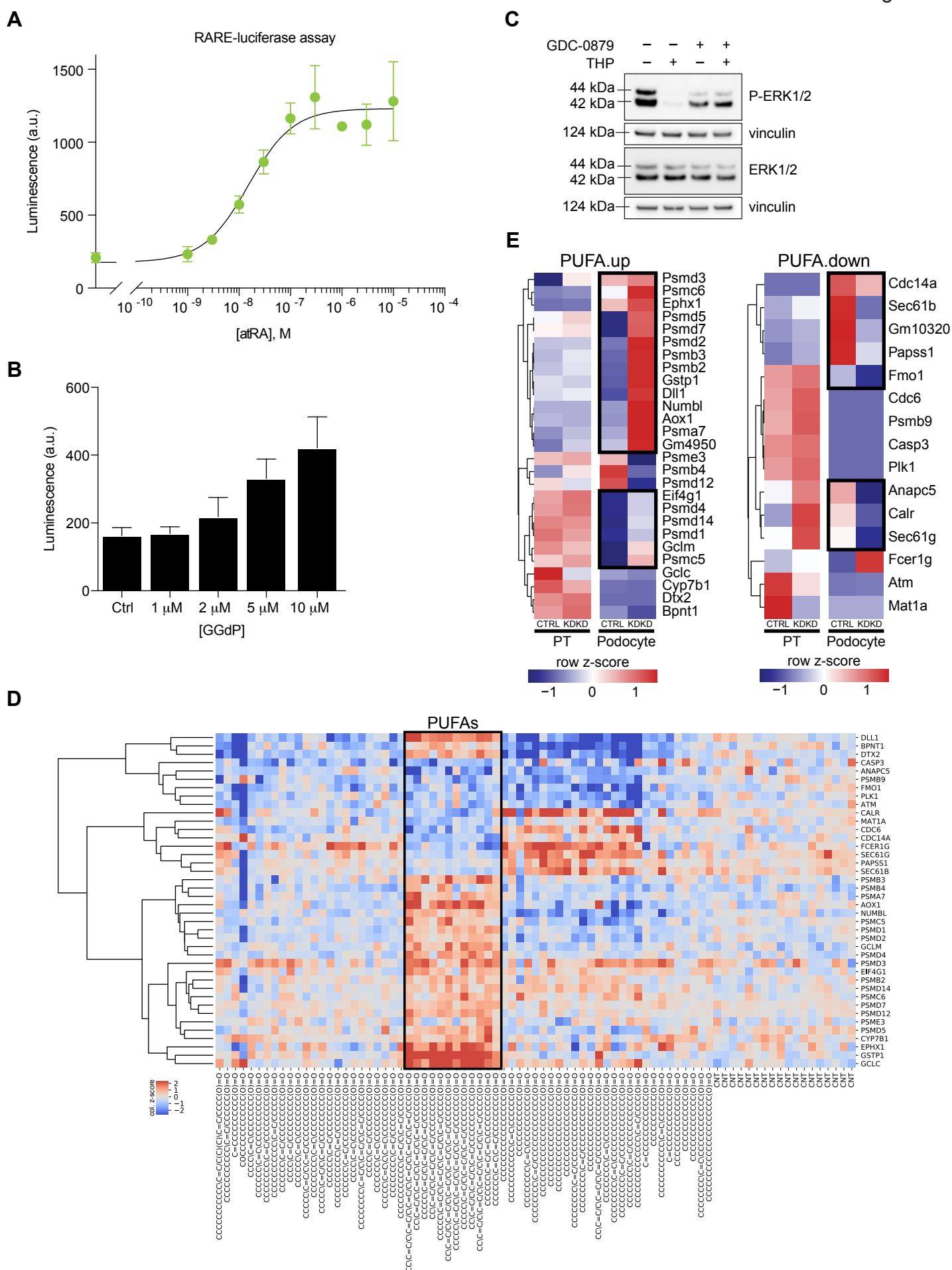
Figure S8. GGdP increases Rar-mediated transcription in a dose-responsive manner, CoQ-deficient mice reveal podocyte-specific changes in PUFA-related genes, and Gpx4 immunofluorescence quantification.
A,B. Luminescence readout from a Retinoic Acid Receptor Element (RARE)-luciferase reporter assay following 24 hours treatment with **A.** atRA, n=3 or **B.** GGdP, n=6, showing that both increase Rar-mediated transcription in a dose-responsive manner. **C.** Western blot of phospho-ERK1/2 (P-ERK1/2) and total ERK1/2 which shows decreased ERK1/2 phosphorylation following treatment with thapsigargin (2.5 μM) and reversed with GDC-0879 (10 μM). **D.** Heatmap of average gene expression of genes used to create PUFA transcriptomic signatures in original dataset of 61 free fatty acids in MIN6 cells, demonstrating selected genes are either up- or down-regulated specifically among PUFAs. **E.** Heatmap of average gene expression of genes used to create the PUFA upregulated gene signature (PUFA up) and PUFA downregulated gene signature (PUFA down) across podocyte and combined proximal tubule cells in control versus *Pdss2kd/kd* mice.
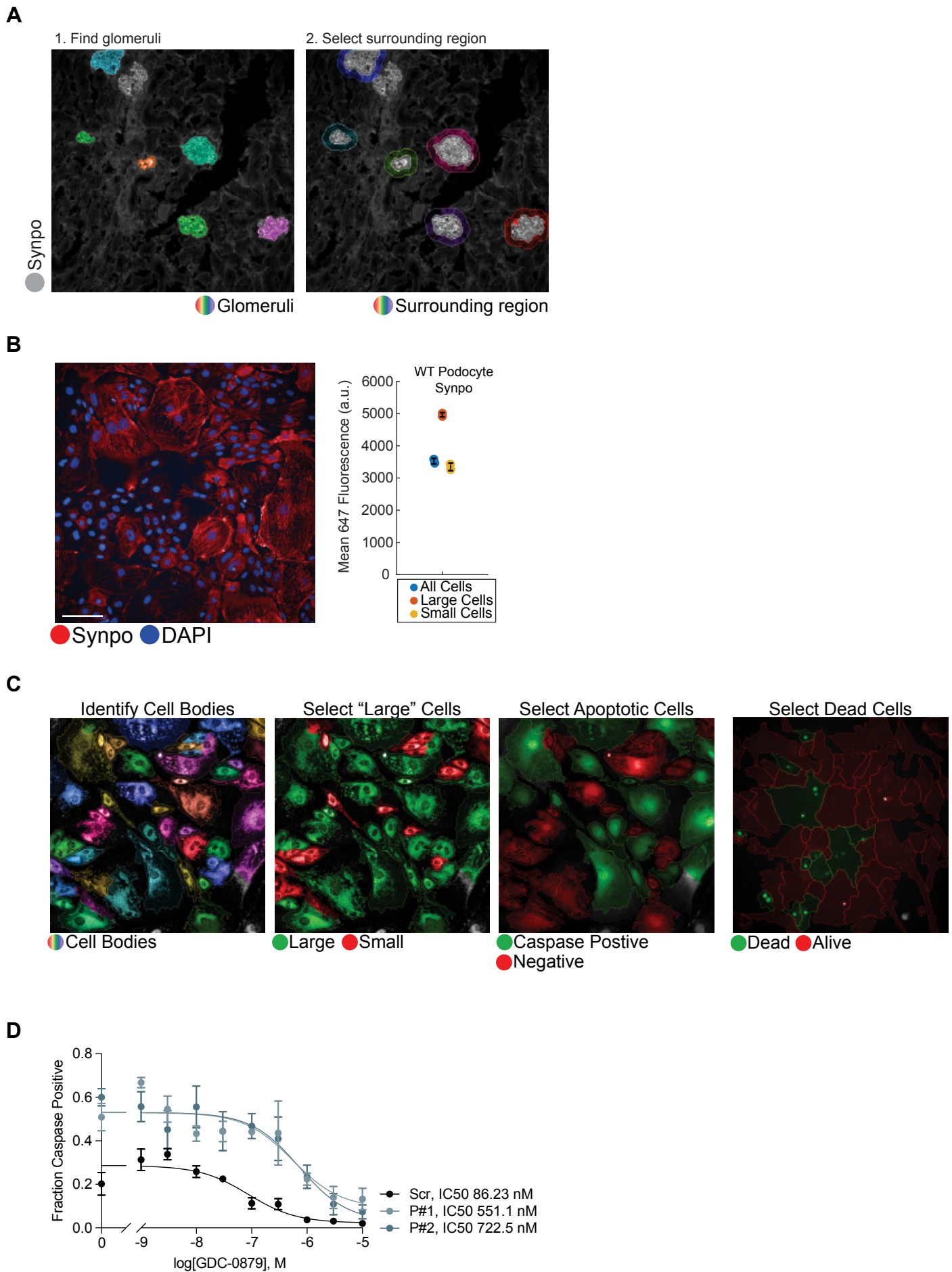
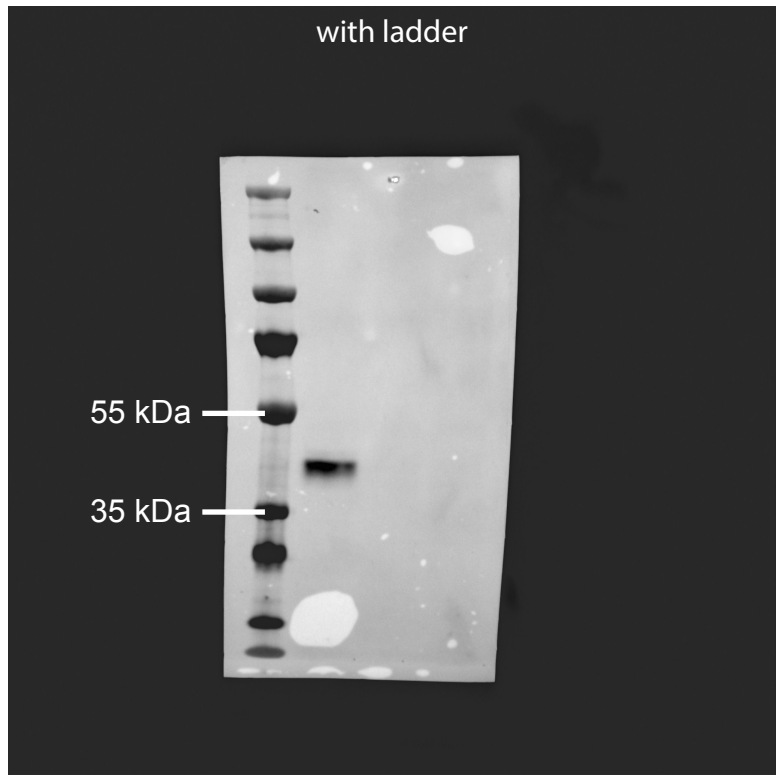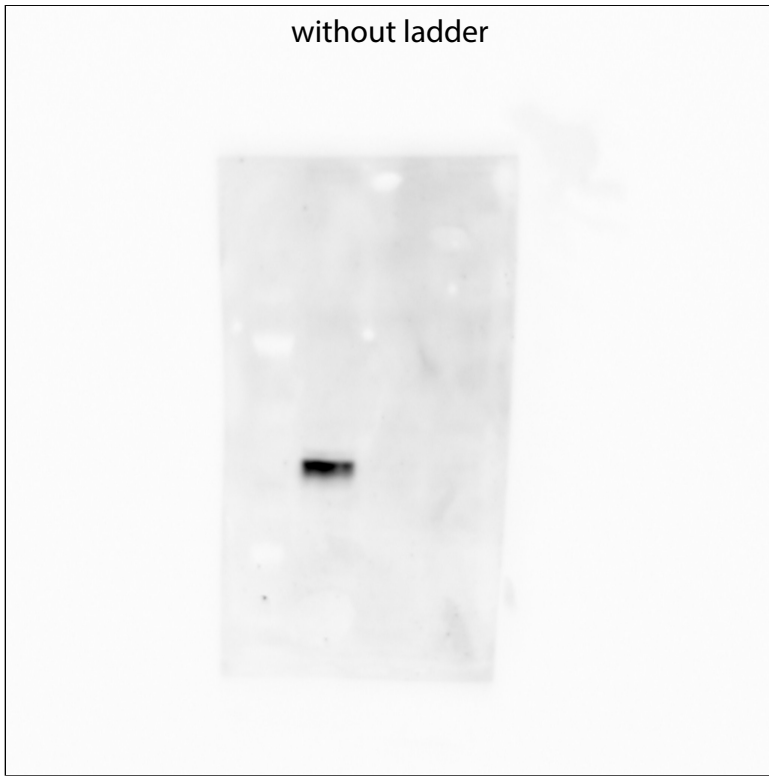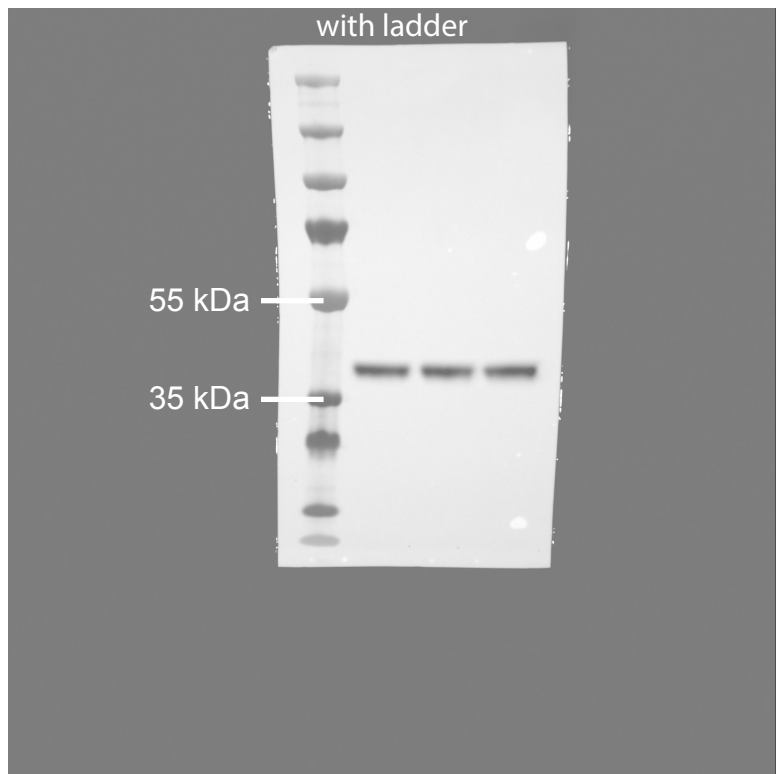**Figure S9. Image analysis using Opera Phenix High-Content Screening System and Harmony software.**
A. Analysis of immunofluorescence by Harmony software demonstrating identification of glomeruli, based on Synpo expression, and surrounding regions for Gpx4 quantification. **B.** Immunofluorescence of synaptopodin (Synpo, red) with nuclei staining (DAPI, blue) and quantification by cell size showing larger cells have increased expression of synaptopodin (SYNPO) suggesting further podocyte maturation; scale bars, 100 μm. **C.** Analysis of live cell imaging by Harmony software demonstrating identification of cell bodies, selection of cells based on size, and selection of apop-totic (caspase positive) and dead cells. **D.** Dose-response curve for GDC-0879 inhibition of podocyte apoptosis in vitro, n=4, IC50 for each condition determined using a nonlinear least squares fit.
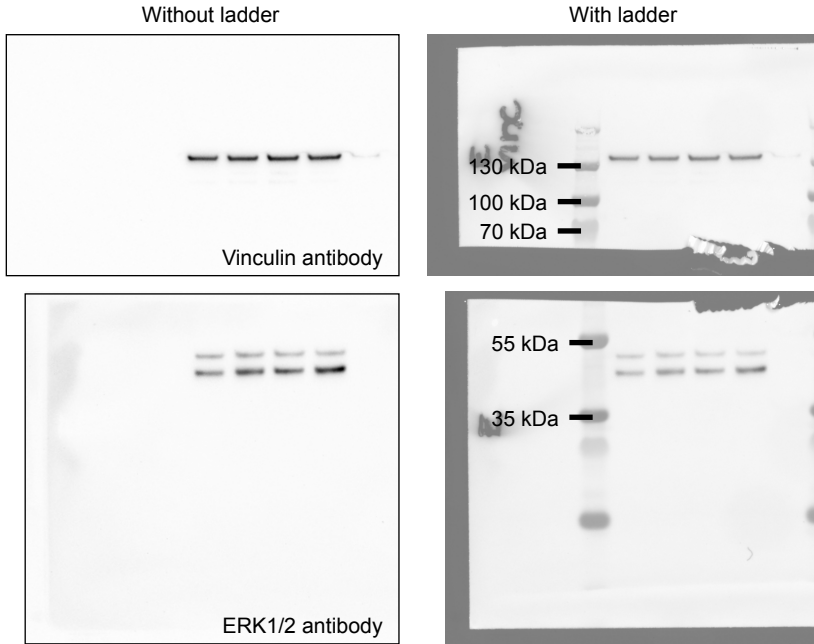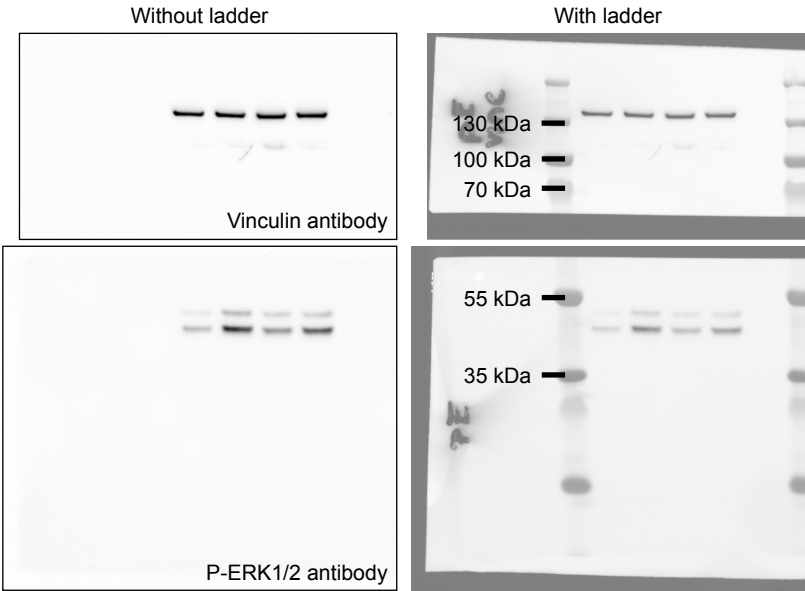
Full unedited Gel for Figure S6A

Pdss2 antibody

without ladder

with ladder

55 kDa

35 kDa

Gapdh antibody

without ladder

with ladder

55 kDa

35 kDa

Full unedited Gels for Figure 4G

Without ladder

With ladder

Vinculin antibody

130 kDa
100 kDa
70 kDa

P-ERK1/2 antibody

55 kDa

35 kDa

Without ladder

With ladder

Vinculin antibody

130 kDa
100 kDa
70 kDa

ERK1/2 antibody

55 kDa

35 kDa

Full unedited Gels for Figure S8C

Without ladder

Vinculin antibody

With ladder

130 kDa
100 kDa
70 kDa

P-ERK1/2 antibody

55 kDa

35 kDa

17e19e

Without ladder

Vinculin antibody

With ladder

17e19e

130 kDa
100 kDa
70 kDa

ERK1/2 antibody

55 kDa

35 kDa